

Nanodiamond dust and the energy distribution of quasars

L. BINETTE¹, A. C. ANDERSEN², H. MUTSCHKE³, and S. HARO-CORZO¹

¹ Instituto de Astronomía, Universidad Nacional Autónoma de México, Apartado Postal 70-264, 04510 México, DF, Mexico

² Dark Cosmology Center, Juliane Maries Vej 30, DK-2100 Copenhagen, Denmark

³ Astrophysikalisches Institut und Universitäts-Sternwarte (AIU), Schillergäßchen 3, D-07745 Jena, Germany

the date of receipt and acceptance should be inserted later

Abstract. The spectral energy distribution of quasars shows a sharp steepening of the continuum shortward of $\simeq 1100 \text{ \AA}$. The steepening could be a result of dust absorption. We present a dust extinction model which considers crystalline carbon grains and compare it with SMC-like dust extinction consisting of a mixture of silicate grains with graphite or amorphous carbon grains. We show that the sharp break seen in *individual* quasar spectra of intermediate redshift $\sim 1\text{--}2$ can be reproduced by dust absorption provided the extinction curve consists of nanodiamonds, composed of terrestrial cubic diamonds or of diamonds similar to the presolar nanodiamonds found in primitive meteorites.

Key words: ISM: dust – GALAXIES: active – ultraviolet emission

©0000 WILEY-VCH Verlag GmbH & Co. KGaA, Weinheim

1. Introduction

The ultraviolet energy distribution of quasars is characterized by the so-called “big blue bump”, which peaks in νF_ν at approximately 1000 \AA . The quasar ‘composite’ spectral energy distribution (SED) of Telfer et al. (2002, hereafter TZ02) obtained by co-adding 332 HST-FOS archived spectra of 184 quasars between redshifts 0.33 and 3.6, exhibits a steepening of the continuum at $\sim 1100 \text{ \AA}$. A fit of this composite SED using a broken powerlaw reveals that the powerlaw index changes from -0.69 in the near-UV to -1.76 in the far-UV (see TZ02). We label this observed sharp steepening the ‘far-UV break’. In these proceedings, we compare the dust absorption that results from nanodiamonds with that of more traditional dust species. In a previous proceedings (Binette et al. 2005b), we described how we came to consider the possibility of carbon crystalline dust. The argumentation in support of the dust absorption interpretation of the UV break has been fully described in Binette et al. (2005a, hereafter BM05). Complementary information about crystalline dust can be found in this and other proceedings (Binette et al. 2005b, 2005c).

2. Dust extinction model

Nanodiamonds are the most abundant presolar grain type found in the relatively unprocessed meteorites, called carbonaceous chondrites. The diamonds account for about 3% of the total amount of carbon in this type of meteorites! The main difference between meteoritic diamonds and cubic terrestrial diamonds is that meteoritic diamonds possess surface impurities that significantly alter their optical properties. This can be appreciated in Fig. 1 where we compare the extinction cross-section resulting from cubic terrestrial diamonds (black continuous line) with that from nanodiamonds from the Allende meteorite (gray continuous line). In both dust models, we assume a powerlaw grain size distribution of index -3.5 bounded by size limits of 2 and 25 \AA . We assume the grains to be spherical and adopt the Mie theory (Bohren and Huffman 1983) and the complex refraction indices $n + ik$ of Mutschke et al. (2004) (for the Allende nanodiamonds) and Edwards & Philipp (1985) (for the terrestrial diamonds). It turns out that within the above small grain size regime, using a log-normal distribution or altering the above grain size limits slightly, do not produce any differences in the derived extinction curves, as explained in BM05.

It is apparent from Fig. 1 that the steepness of the *near-UV* extinction rise in the case of nanodiamonds ought to produce a sharp absorption break, a desired feature for any dust model that aims at fitting the UV quasar break. The nanodiamond extinction curves in Fig. 1 were normalized in such a

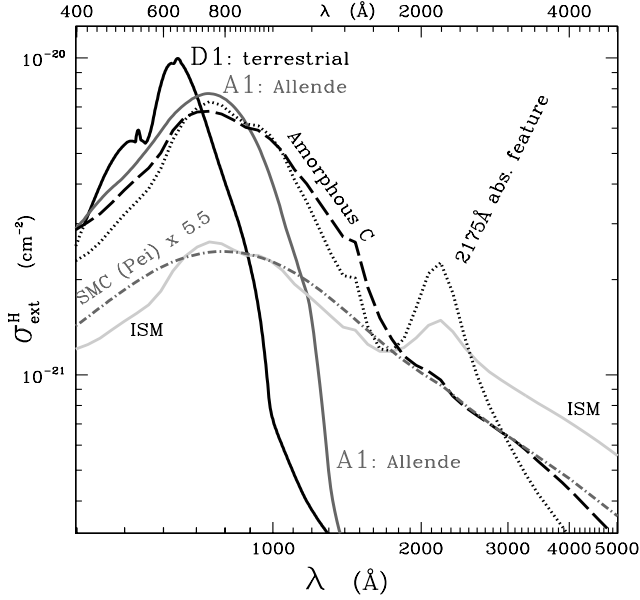


Fig. 1. Extinction cross section for terrestrial cubic nanodiamonds (black continuous line labeled D1) and meteoritic nanodiamonds from the Allende Meteorite (gray continuous line labeled A1). The silver continuous line represents a graphite and silicate model of the ISM dust by Martin & Rouleau (1991), with grain sizes ranging from 50 to 2500 Å. The dotted line corresponds to a similar (ISM) grain composition but with sizes confined to the range 50 to 300 Å. Notice the graphite absorption feature at 2175 Å in both curves. The long dashed line describes a dust model consisting of grains composed of silicate (50%), amorphous carbon (45%) and 5% of graphite, with grain sizes within the range 50 to 300 Å. The dot-dashed gray line represents the SMC dust model of Pei (1992) multiplied here by the factor 5.5.

way that they represent the case of having all the carbon in the dust (assuming a solar C/H abundance ratio). This normalization would need to be scaled according to the actual but unknown dust-to-gas ratio appropriate to the quasar environment.

3. Powerlaws absorbed by nanodiamond dust

In BM05, we present calculations in which the dust is either intrinsic to the quasars or intergalactic. In the end, we concluded that only the *intrinsic dust* hypothesis was satisfactory. The calculations presented here will assume the intrinsic dust case, which requires gas columns of order 10^{20} cm^{-2} assuming Solar carbon abundance and full depletion onto nanodiamond grains.

Both nanodiamond types can produce a sharp UV break as shown in Fig. 2 where we assumed a powerlaw energy distribution of spectral index -0.40 (dotted line) and a column of 10^{20} cm^{-2} . The opacity is given by $\tau_{\lambda}^{ext} = N_H \sigma_{ext}^H(\lambda)$ and the transmission function is simply $e^{-\tau_{\lambda}^{ext}}$. It is interesting to notice that the break in the absorbed powerlaws in Fig. 2 is shortward (longward) of Ly α in the case of cubic diamonds (meteoritic nanodiamonds), respectively.

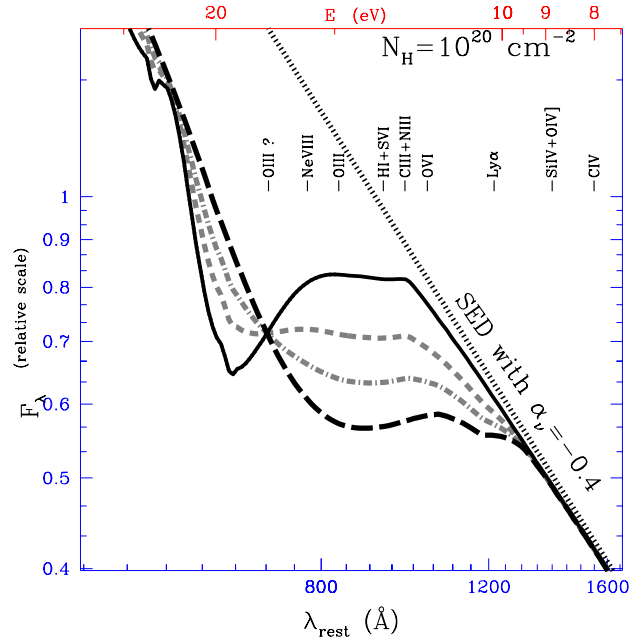


Fig. 2. Absorption models assuming a powerlaw SED of index $\alpha_{\nu} = -0.4$ (dotted line). The nanodiamond dust screen corresponds to a hydrogen column of 10^{20} cm^{-2} . The absorbed SED represented by the continuous line corresponds to the extinction by terrestrial cubic diamonds (D1), while the long dashed line corresponds to nanodiamonds from the Allende meteorite (A1). The gray lines correspond to a mixture of the two flavors: dashed line: 60% D1 + 40% A1, dot-dashed line: 30% D1 + 70% A1. Labelled pointers indicate where emission lines are expected in the rest-frame quasar spectra.

It turns out that the UV break position in most spectra is about midway between the break positions produced by either of the two nanodiamond types, suggesting that a combination of both types is needed, as described in more detail in BM05. We found that most quasar spectra favor a composition consisting on the order of 30% of cubic diamonds and 70% of meteoritic nanodiamonds. In Fig. 3a, we illustrate the effect of varying the absorption column N_H , assuming the above mixture (30% and 70%, respectively, equivalent to $f_{D1} = 0.3$). The curves shown correspond to the four H columns values of $N_{20} = 0.5, 1.0, 2.0$ and 4.0 , in units of 10^{20} cm^{-2} . The same powerlaw SED (dotted line) is assumed as for Fig. 2, that is $\alpha_{\nu} = -0.4$.

4. Comparison with SMC-like dust

Can ISM or SMC-like dust reproduce the quasar break? According to Shang et al. (2005), reddening by ISM or SMC-like grains “is not able to produce the spectral break seen in the AGN sample, without leaving a clear signature at longer wavelengths”. Instead of a sharp break, ISM extinction results in a shallow rollover that extends in the near-UV and even in the optical domain. In the HST-FOS sample that we studied, most spectra (the 50 class A and B spectra) are quite hard in the near-UV, consistent with a powerlaw continuum

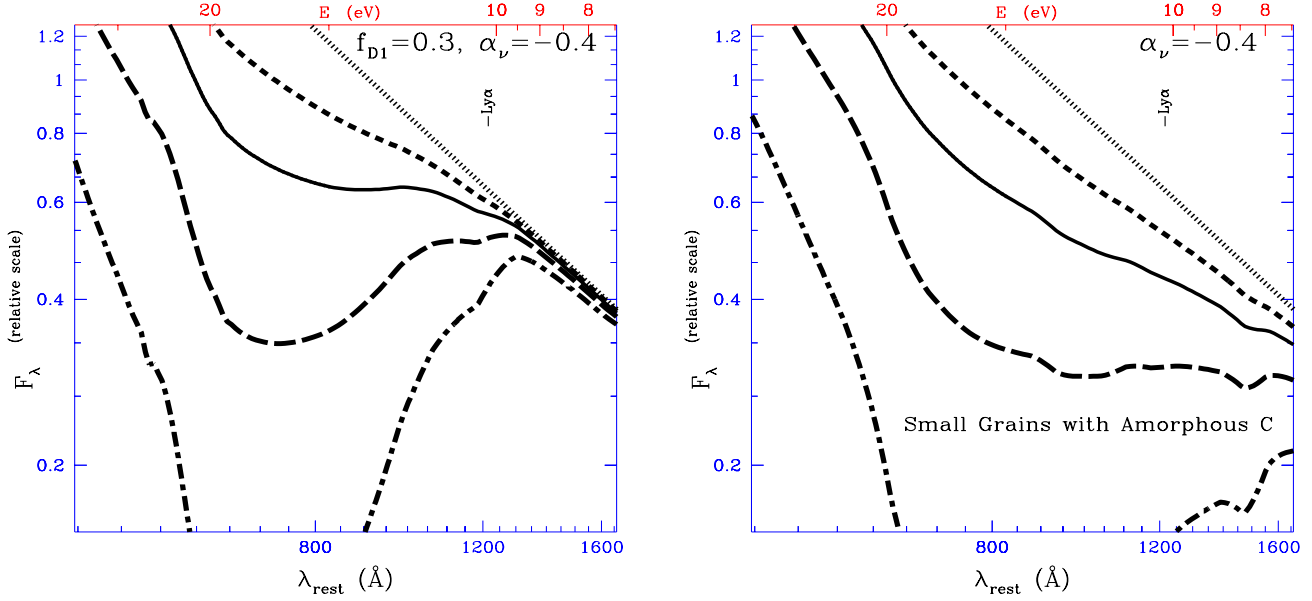


Fig. 3. Absorbed powerlaw SED of index $\alpha_\nu = -0.4$ (dotted line) for the following N_H columns in units of 10^{20} cm^{-2} : $N_{20} = 0.5$ (dashed line), 1.0 (solid line), 2.0 (long dashed line) and 4.0 (dash-dot line). The following two dust compositions are considered. Panel a (left): the dust corresponds to a combination of terrestrial cubic diamonds (30%) and primitive meteorite nanodiamonds (70%). Panel b (right): the dust grains are made of silicate (50%), amorphous carbon (45%) and graphite (5%).

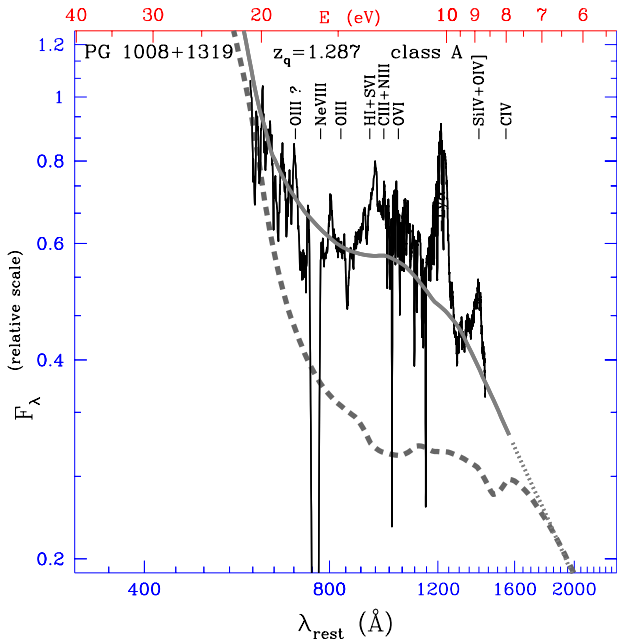


Fig. 4. The rest-frame spectrum of class (A) quasar PG 1008+1319. Notice the far-UV rise shortward of the UV break. The nanodiamond dust extinction model (gray continuous line) assumes a powerlaw with $\alpha_\nu = +0.13$ (from Neugebauer et al. 1987), $N_{20} = 1.2$ and the same dust composition as in Fig. 3a (mixed nanodiamond types). The gray dashed line corresponds to extinction by silicate-amorphous carbon dust (as in Fig. 3b) assuming a column $N_{20} = 2.4$. The transmitted flux in the latter model has been multiplied by 1.3 so that longward of 1800 Å it superimposes the transmitted flux of the nanodiamond model.

longward of 1100 Å. They do not indicate any substantial reddening longward of the break (except the 8 objects associated to class C, see BM05). In Fig. 1, the extinction cross-section resulting from ISM dust is represented by the silver continuous line. The model depicted consists of silicate and graphite grains with grain sizes ranging between 50 and 2500 Å.

The extinction by SMC-like dust, however, is more peaky in the near-UV and, as will be shown, cannot reproduce the sharp 1000 Å break either. For comparison, the long dashed line in Fig. 1 represents the cross-section of a dust model consisting of relatively small grain sizes, ranging from 3 to 300 Å, but with graphite replaced by amorphous carbon (using results from Rouleau & Martin 1991), that is, dust composed of 50% silicate grains, 45% amorphous C grains and 5% graphite grains. The dust-to-gas ratio is the same as for the Galactic ISM model. The reason for replacing most of the ‘usual’ graphite grains by amorphous carbon is guided by the need to remove the 2175 Å absorption feature present when small graphite grains are abundant. Our aim is to test an extinction curve that would be SMC-like, in accordance with the extinction law inferred from the SLOAN quasar sample by Richards et al. (2003), Hopkins et al. (2004) and Willott (2005). In Fig 3, we indicate how the previous powerlaw SED would look if absorbed by dust containing silicates and amorphous carbon (corresponding to the long dashed line extinction model in Fig. 1), for the four columns values of $N_{20} = 0.5, 1.0, 2.0$ and 4.0, in units of 10^{20} cm^{-2} . A sharp break does occur for columns $N_{20} \sim 2$. The break takes place, however, at too long a wavelength in the near-UV. This is illustrated in Fig 4 where we compare the spectra of PG 1008+1319 with a powerlaw absorbed by nanodiamonds (gray continuous line) and by silicate-amorphous carbon dust

(gray dash line). Clearly, only the nanodiamond dust provides a satisfactory fit.

Adopting the more commonly used SMC dust model of Pei (1992), which consists only of silicate grains, would not improve the situation, since the extinction cross-section is even shallower in the near-UV in the Pei model than in the case of the silicate-amorphous carbon dust. A comparison of these two extinction curves is made in Fig. 1. The Pei cross-section has been multiplied by 5.5 (Fig. 1) to show that it approximately overlaps in the range 1800–5000 Å with the silicate-amorphous C extinction curve. This confirms that the selective extinction of both dust models is quite comparable in the optical domain.

5. Conclusion

Dust absorption by nanodiamonds is successful in reproducing the 1000 Å break as well as the far-UV rise seen at shorter wavelengths in distant quasars. To confirm the possible existence of nanodiamond grains in quasars, observations of the far-infrared emission bands caused by hydrogenated nanodiamonds (van Kerckhoven et al. 2002; Jones et al. 2004) could be attempted or, alternatively, one may try to confirm a flux rise shortward of 700 Å for as many quasars as possible. The latter would require high quality far-UV sensitive observations, which will hopefully be provided by the World Space Observatory satellite (Barstow et al. 2003).

The model presented is successful in both fitting the breaks shape and the position of, as well as in reproducing the sharp flux recovery observed in key quasar spectra, around 660 Å. While very high redshift quasars ($z \gtrsim 2.5$) appear not to be absorbed by dust, their energy distribution suggests the existence of a higher energy continuum rollover at $\simeq 670$ Å. As shown in BM05, when such a break is incorporated into the description of the energy distribution of all quasars, the dust absorption model can account for the overall shape of the 'composite' spectral energy distribution of the 184 quasars constructed by TZ02.

Acknowledgements. The authors acknowledge support from CONACyT grant 40096-F. HM acknowledges support by DFG grant Mu1164/5. We thank Randal Telfer for sharing the reduced HST-FOS spectra and Diethild Starkmeth for proof reading.

References

- Barstow, M. A., Binette, L., Brosch, N., Cheng, F. Z., Dennefeld, M., de Castro, A. I. G., Haubold, H., van der Hucht, K. A., Kappellmann, N., Martinez, P., Moiseev, A., Pagano, I., Ribak, Erez N., Sahade, J., Shustov, B. I., Solheim, J.-E., Wamsteker, W., Werner, K., Becker-Ross, H., Florek, S.: 2003, *Proc. SPIE* 4854, 364
- Binette, L., Magris C., G., Krongold, Y., Morisset, C., Haro-Corzo, S., de Diego, J. A., Mutschke, H., Andersen, A.: 2005a, *ApJ* 631, 661 (BM05)
- Binette, L., Morisset, C., Haro-Corzo, S.: 2005, in *proc. of The ninth Texas-Mexico Conference on Astrophysics*, April 13–16, 2005, in San Antonio, Texas, eds. S. Torres and G. MacAlpine, *RevMexAA (Conf. Ser.)* in press

- Binette, L., Krongold, Y., Magris C., G., de Diego, J. A.: 2005b, in *proc. of "Triggering relativistic jets"* held in Cozumel, 28 March – 1 April 2005, Eds. W. Lee and E. Ramirez-Ruiz, *RevMexAA (Conf. Ser.)* in press
- Bohren, C. F., Huffman, D.R.: 1983, *Absorption by Small Particles* (New York: Wiley)
- Edwards, D. F., Philipp, H. R.: 1985, in *Handbook of Optical Constants of Solids*, ed. E. D. Palik (Orlando: Academic Press), p. 665
- Hopkins, P. F., et al.: 2004, *AJ* 128, 1112
- Jones, A. P., d'Hendecourt, L. B.: 2004, in *ASP Conf. Series, Astrophysics of Dust*, V. 309, p. 589
- Martin, P. G., Rouleau, F.: 1991, *Extreme Ultraviolet Astronomy*, ed. R.F. Malina and S. Bowyer (Pergamon, Oxford), p. 341
- Mutschke, H., Andersen, A. C., Jäger, C., Henning, T., Braatz, A.: 2004, *A&A* 423, 983
- Neugebauer, G., Green, R. F., Matthews, K., Schmidt, M., Soifer, B. T., Bennett, J.: 1987, *ApJS* 63, 615
- Pei, Y. C.: 1992, *ApJ* 395, 130
- Richards, G. T., et al.: 2003, *AJ* 126, 1131
- Rouleau, F., Martin, P. G.: 1991, *ApJ* 377, 526
- Shang, Z., Brotherton, M. S., Green, R. F., Kriss, G. A., Scott, J., Quijano, J. K., Blaes, O., Hubeny, I., Hutchings, J., Kaiser, M. E., Koratkar, A., Oegerle, W., Zheng, W.: 2005, *ApJ* 619, 41
- Telfer, R. C., Zheng, W., Kriss, G. A., Davidsen, A. F.: 2002, *ApJ* 565, 773 (TZ02)
- van Kerckhoven, C., Tielens, A. G. G. M., Waelkens, C.: 2002, *A&A* 384, 568
- Willott, C. J.: 2005, *ApJ* in press, arXiv:astro-ph/0505446